Article

Lithium Salt of 2,5-Bis(trimethylsilyl)stannolyl Anion: Synthesis, Structure, and Nonaromatic Character

Kohei Kitamura [1], Youichi Ishii [1] and Takuya Kuwabara [2],*

[1] Department of Applied Chemistry, Faculty of Science and Engineering, Chuo University, 1-13-27, Kasuga, Bunkyo-ku, Tokyo 112-8551, Japan
[2] Department of Chemistry and Biochemistry, Graduate School of Humanities and Sciences, Ochanomizu University, 2-1-1, Otsuka, Bunkyo-ku, Tokyo 112-8610, Japan
* Correspondence: kuwabara.takuya@ocha.ac.jp

Abstract: The aromatic character of silolyl and germolyl anions markedly depends on the substituents in the 2,5-positions; carbon-substituted derivatives are nonaromatic, whereas silyl-substituted ones tend to exhibit an aromatic character. However, only carbon-substituted derivatives have been reported for stannolyl anions. In this study, we present the synthesis and structure of a 2,5-disilylated stannolyl anion. Transmetalation of a 2,5-disilyl-1-zirconacyclopentadiene with $SnCl_4$ gave a dichlorostannole **1**, which reacted with potassium tris(trimethylsilyl)silanide to introduce a bulky silyl group on the tin atom. Reduction of the 1-chloro-1-silylstannole **2** with lithium generated the lithium salt of the desired stannolyl anion **3** that adopts an η^1-coordination to the lithium atom. We concluded that the stannolyl anion **3** is nonaromatic based on the pyramidalized tin center and the C–C bond alternation in the five-membered ring as well as the NMR properties.

Keywords: stannolyl anion; aromaticity; metallole; substituent effect

1. Introduction

Heavier congeners of cyclopentadienyl anions, known as metallolyl anions and dianions with general formulas of $[C_4R_5E]^-$ and $[C_4R_4E]^{2-}$ (E = Si, Ge, Sn, Pb), respectively, have attracted continuous attention as novel ligands in coordination chemistry and unconventional aromatic systems consisting of heavier group 14 elements [1–4]. Following the seminal works by Tilley on the coordination chemistry of silolyl/germolyl anions and dianions [5–10], several groups have contributed to the development of this field. Various transition metal complexes incorporating metallolyl ligands have been reported, exhibiting diverse coordination modes such as μ-η^5:η^5- [11,12], η^5- (**I** in Figure 1) [13], μ-η^1:η^1- (**II**) [14,15], μ-η^1:η^5- [16], η^1- [17], and η^4-like fashions [13,18]. Recently, the coordination chemistry of metallolyl dianions towards rare-earth elements and f-block metals has also been investigated [19–22]. These studies have shown that η^5-coordinating metallolyl anions and dianions are aromatic with almost equal C–C bonds in the five-membered ring, whereas η^1- and η^4-coordinating ones are nonaromatic with a 1,3-diene character [14]. Therefore, coordinating modes have a significant impact on the electronic structure of metallolyl anions and dianions.

The aromaticity of alkali metal salts of metallolyl anions and dianions is also an important topic in this field. The family of group 14 metallole dianions (silole [23–26], germole [26–28], stannole [29–31], and plumbole [32,33]) has been concluded to be aromatic (**III**). In contrast, the situation is more complicated in metallolyl monoanions. In the 1990s, silolyl and germolyl anions with the formula of $[C_4Me_4ER]^-$ (E = Si, Ge; R = Me, Mes (2,4,6-trimethylphenyl), $SiMe_3$) have been structurally characterized, which revealed the pyramidal metal center and bond-altered five-membered ring (**IV**) [34]. Because this trend is also found in the structures of stannolyl and plumbolyl anions $[C_4Ph_4ER]^-$ (E = Sn, Pb; R = Ph,

Mes, SiMe$_3$) [32,35], the family of metallolyl anions was concluded to be nonaromatic. However, more recently, Kovács, Nyulászi, et al. demonstrated theoretically and experimentally that the lithium salt of silolyl anion, which has silyl substituents on the alpha-carbon atoms (C$_\alpha$: 2,5-positions in the silole ring), is aromatic with an η^5-coordination and a planar three-coordinated silicon center (**V**) [36,37]. Furthermore, Müller's group reported a potassium salt of a 2,5-disilylgermolyl anion that exhibits an aromatic/nonaromatic switch depending on the coordinating solvent to the potassium ion; the THF-solvated salt has an aromatic character with an η^5-coordination, while the corresponding 18-crown-6 ether adduct is nonaromatic with an η^1-coordination as well as a pyramidal germanium center [38].
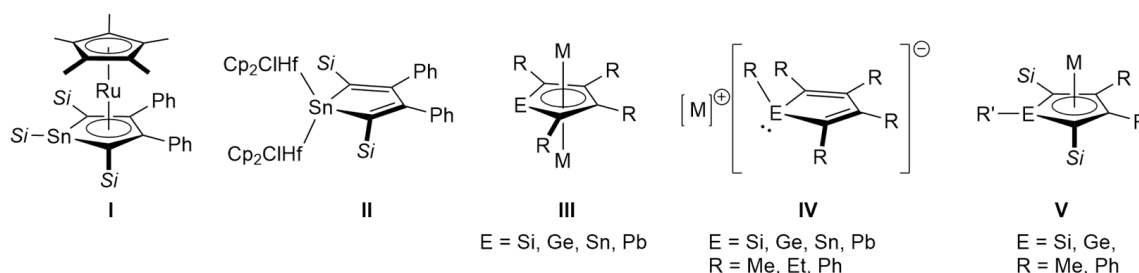

Figure 1. Selected metallolyl complexes (**I**,**II**), alkali metal salts of metallolyl dianions (**III**), nonaromatic metallolyl anions (**IV**), and aromatic metallolyl anions (**V**). The substituents *Si* and M indicate trialkylsilyl groups and alkali metals, respectively.

This effect of the silyl substituents, which imparts aromatic character to silolyl and germolyl anions, originates from the effective hyperconjugation (σ^*–π interaction) between the trialkylsilyl groups and the anionic π-electron system [38], raising the possibility of realizing aromatic stannolyl anions. To date, only the tetraphenyl- and tetraethyl stannolyl anions [C$_4$Ph$_4$SnR]$^-$ and [C$_4$Et$_4$SnR]$^-$ have been structurally characterized. These two derivatives are nonaromatic with a highly pyramidal tin center, like **IV** [30]. In this report, we present the synthesis and structural analysis of a lithium salt of 2,5-disilylated stannolyl anion. X-ray diffraction studies and NMR spectroscopic analysis indicate that the stannolyl anion is nonaromatic rather than aromatic, despite the assistance of the silyl groups.

2. Results and Discussion

Scheme 1 shows the synthetic route to the target stannolyl anion. Although synthetic examples of 1,1-dichlorostannole are limited [39,40], dichlorostannole **1** is expected to be a suitable precursor. Initial attempts to synthesize **1** from the reaction of the corresponding 1,4-dilithiobutadiene, which was prepared by the reduction of 1-(trimethylsilyl)-1-propyne with lithium, and SnCl$_4$ were unsuccessful. Accordingly, CuCl-promoted transmetalation of an in situ generated zirconacycle [41] and SnCl$_4$ was investigated. Although the tin source for this transformation described in the literature has been limited to R$_2$SnX$_2$, where R = alkyl or aryl and X = halogen [42], dichlorostannole **1** was successfully obtained by this method in a 58% yield. Treatment of **1** with a potassium salt of tris(trimethylsilyl)silanide provided chlorostannole **2** with a bulky silyl group on the tin atom. Reduction of **2** with lithium in Et$_2$O, followed by recrystallization from hexane–THF, provided a lithium salt of stannolyl anion **3·(thf)$_3$** as highly air- and moisture sensitive orange crystals. On drying the crystals in vacuo, **3·(thf)$_3$** released two of the three THF molecules to provide **3·(thf)** in a 26% isolated yield. These new compounds were characterized using ^{1}H and multinuclear NMR spectroscopy, elemental analysis (excluding **3·(thf)**), and X-ray diffraction analysis (excluding **1**). Considering that the mono-THF solvated germolyl anion reported by Müller et al. has an aromatic character with a planar germanium atom [38], it is inferred that **3·(thf)** may have a potential aromatic character. Unfortunately, our attempts to obtain single crystals of **3·(thf)** from its toluene and benzene solution were unsuccessful. However, NMR data of **3·(thf)** recorded in C$_6$D$_6$ suggests that **3·(thf)** is nonaromatic at least in solution (*vide infra*).
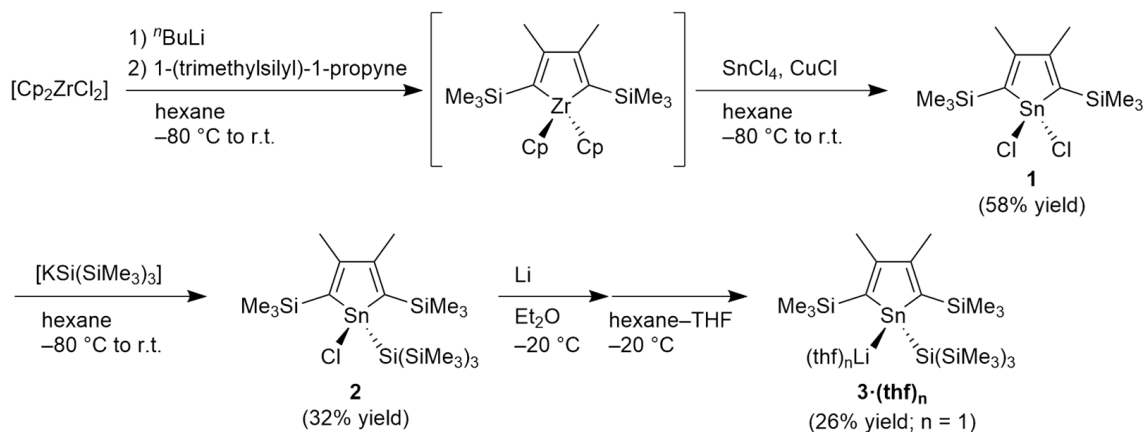
Scheme 1. Synthetic procedure for lithium salt of stannolyl anion **3**.

Figure 2 illustrates the solid-state structures of **2** and **3·(thf)₃** determined by X-ray diffraction analysis, and Table 1 highlights the structural differences between **2**, **3**, and a previously reported stannolyl anion isolated as a solvent-separated ion pair [Li(12-c-4)][C₄Ph₄Sn(SiMe₃)] **4**, where 12-c-4 indicates 12-crown-4 ether [35].
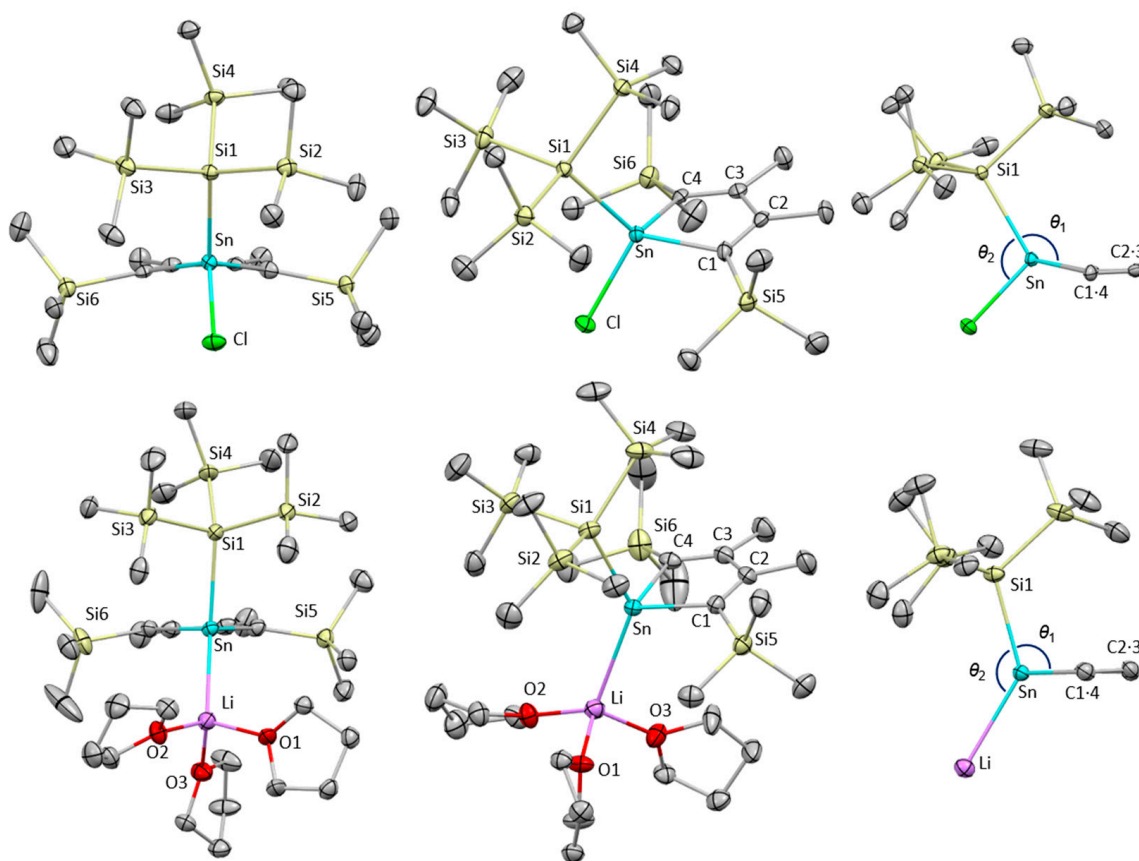
Figure 2. Molecular structures of one of the three independent molecules of **2** (**top**) and **3·(thf)₃** (**bottom**) with thermal ellipsoid plots at 50% probability. All hydrogen atoms are omitted for clarity. θ_1 and θ_2 are the angles of Si1−Sn−C$_{center}$ and Si1−Sn−Cl(Li), respectively (C$_{center}$ is the midpoint of C1 and C4 atoms).

Table 1. Selected bond lengths [Å] and angles [°].

Bonds and Angles [1]	2 [2]	3·(thf)$_3$	4 [3]
Sn−C1, Sn−C4 [3]	2.163, 2.151	2.197(3), 2.202(3)	2.197(4), 2.198(4)
C1−C2, C3−C4	1.352, 1.352	1.362(4), 1.363(4)	1.360(6), 1.350(6)
C2−C3	1.521	1.489(4)	1.498(6)
Sn−Si	2.589	2.6586(8)	2.6154(14)
C1−Sn−C4	85.6	81.33(10)	78.56(15)
θ_1	132.5	103.9	89.6
θ_2	109.2	134.16(10)	–

[1] See Figure 1 for the atom labels, θ_1, and θ_2. [2] Average values for the three independent molecules are shown. [3] Data from Ref. [35].

The asymmetric unit of **2** contains three independent molecules, each with slightly different metrical parameters. The tin and Si5/6 atoms deviate by 0.3 and 0.26–0.41 Å from the least-squares plane defined by C1–C4 atoms due to the steric repulsion between the bulky tris(trimethyl)silyl and trimethylsilyl groups. The average Sn−C1 and Sn−C4 bond lengths are 2.163 and 2.151 Å, which are slightly longer than those in sterically less hindered stannoles (2.1357(18) and 2.134(3) Å) [30,31]. The C−C bonds in the five-membered ring are clearly altered (1.352, 1.521, and 1.352 Å), indicating its 1,3-diene character. In the packing structure, the stannole molecules are well aligned along the *b*-axis, as shown in Figure S1. At present, we infer that the well-ordered structure is realized by multiple weak hydrogen bonds between the CH groups of the Si(SiMe$_3$)$_3$ and the chlorine atom because the interatomic distances of the CH⋯Cl (approximately 3.1–3.5 Å) fall into a range of CH⋯Cl hydrogen bond lengths [43].

Lithium salt of stannolyl anion **3·(thf)$_3$** crystallizes as a contact ion pair, adopting η^1-coordination to the lithium cation instead of an η^5-fashion. Note that this represents the first example of a contact ion pair of an alkali metal salt of stannolyl anions. The Sn−Li distance is 2.879(5) Å, which falls within the typical range for Sn−Li bonds [44–46]. The 1,3-diene character is confirmed by the C–C bond alternation in the five-membered ring, where the bond lengths of C1–C2, C2–C3, and C3–C4 are 1.362(4), 1.489(4), and 1.363(4) Å, respectively. The Sn−Si bond in **3·(thf)$_3$** (2.6587(8) Å) is longer than that in **2** (2.589(1) Å). The Sn−C1/C4 bonds (2.197(3)/2.202(3) Å) in **3·(thf)$_3$** are also elongated compared to those in **2** (2.148(4)–2.167(4) Å). These structural changes from **2** to **3·(thf)$_3$** are attributed to the negative charge localized on the tin atom; the lone pair with a high s-character increases the p-character of the Sn–Si and Sn–C bonds. Although the bond lengths in **3·(thf)$_3$** and **4** listed in Table 1 resemble each other, the degree of pyramidalization is slightly smaller in **3·(thf)$_3$** (θ_1: 103.9 vs. 89.6°) due to the Sn−Li bond in **3·(thf)$_3$**. This is also confirmed by the sum of the three angles around the tin atom: 282.3° for **3·(thf)$_3$** and 255.1° for **4**. Additionally, the angle θ_2 in **2** (Si1−Sn−Cl) is 109.2°, which is an ideal angle for a tetracoordinated atom (109.5°), whereas the angle in **3·(thf)$_3$** (Si1−Sn−Li) is considerably large (134.16(10)°) due to the high s-character of the tin lone pair.

To understand the structure of **3·(thf)** in solution, NMR studies were performed. Table 2 summarizes the chemical shift changes upon reduction. The ^{119}Sn{^{1}H} NMR signal shifted from δ 101.3 (**2**) to −130.6 (**3·(thf)**), indicating that the negative charge is localized on the tin atom. A similar trend has been reported for related anionic stannacycles [47,48]. On the contrary, the ^{29}Si NMR signal of the aromatic silolyl anion reported by Kovács, Nyulászi, et al. shifted to the lower field compared to that of its neutral precursor (δ 65.7 for the silolyl anion vs. 17.0 for its precursor) due to the π-electron delocalization [36]. A significant downfield shift was observed for the C$_\alpha$ signal [from δ 148.5 (**2**) to 180.2 (**3·(thf)**], as was observed in stannolyl and plumbolyl anions, which can be explained by the substantial contribution of the paramagnetic term (σ_{para}) [49]. In the ^{7}Li NMR spectrum, a slightly broadened signal was observed at δ −1.47. Considering that negatively large ^{7}Li NMR chemical shifts (approximately −4 to −6 ppm) for lithiated metalloles indicate the aromaticity of the metallolyl anions due to the diatropic ring currents [50], we concluded

that **3·(thf)** is also nonaromatic in solution. It is interesting to note that the Me signal of the stannole ring shifted to a lower field upon reduction (from δ 2.01 (**2**) to 2.34 (**3·(thf)**)), despite the negative charge on the stannole ring in **3·(thf)**. Therefore, using the chemical shift of the ring Me signal to diagnose aromaticity in metallolyl anions could lead to mischaracterization.

Table 2. Chemical shift changes upon reduction.

	2	**3·(thf)**	$\Delta(\delta_3 - \delta_2)$
$\delta(^{119}\text{Sn})$	101.3	-130.6	-231.9
$\delta(^{13}\text{C}_\alpha)$	148.5	180.2	31.7
$\delta(^{13}\text{C}_\beta)$	162.0	156.9	-5.1
$\delta(^1\text{H})$ of $\text{C}_\beta-\text{Me}$	2.01	2.34	-0.33

3. Materials and Methods

3.1. General Considerations

All manipulations were carried out under an argon atmosphere using standard Schlenk techniques or a glovebox, unless otherwise stated. Hexane, toluene, Et$_2$O, THF, and C$_6$D$_6$ were distilled over potassium mirror. 1-(Trimethylsilyl)-1-propyne, SnCl$_4$, and [Cp$_2$ZrCl$_2$] were purchased from Tokyo Chemical Industry Co., Ltd. (Fukaya City, Japan), Kanto Chemical Co., Inc. (Tokyo, Japan), and Sigma-Aldrich Chemical Co. (Burlington, MA, USA), respectively. KSi(SiMe$_3$)$_3$ was synthesized according to the literature [51]. ^{1}H (500 MHz), ^{13}C{^{1}H} (125 or 100 MHz), ^{7}Li{^{1}H} (194 MHz), ^{29}Si{^{1}H} (99 MHz), and ^{119}Sn{^{1}H} (186 MHz) NMR spectra were recorded on a JEOL ECA-500 (JEOL Ltd., Tokyo, Japan) or a Varian Mercury 400 spectrometers (International Equipment Trading Ltd., Mundelein, IL, USA) at 20 °C, unless otherwise stated. Chemical shifts are reported in δ and referenced to residual ^{1}H and ^{13}C{^{1}H} signals of deuterated solvents as internal standards or to the ^{7}Li{^{1}H}, ^{29}Si{^{1}H}, and ^{119}Sn{^{1}H} NMR signals of LiCl in D$_2$O (δ = 0.00), SiMe$_4$ in CDCl$_3$ (δ = 0.00), and SnMe$_4$ in C$_6$D$_6$ (δ = 0.00) as external standards. In ^{13}C{^{1}H} NMR data, 1°, 2°, 3°, and 4° represent primary, secondary, tertiary, and quaternary carbons, respectively. Elemental analyses were performed on a Perkin Elmer 2400 series II CHN analyzer (PerkinElmer, Waltham, MA, USA).

3.2. Synthesis of 1,1-Dichloro-2,5-trimethylsilyl-3,4-dimethylstannole **1**

In a Schlenk flask, a suspension of [Cp$_2$ZrCl$_2$] (2.001 g, 6.84 mmol) in hexane (70 mL) was cooled to −80 °C. Then, ^{n}BuLi (1.57 M in hexane, 8.9 mL, 14 mmol) was added dropwise, and the mixture was stirred for 30 min at this temperature. After adding 1-(trimethylsilyl)-1-propyne (2.1 mL, 14 mmol), the mixture was stirred at room temperature for 20 h to give a yellow suspension. The mixture was then cooled to −80 °C, and CuCl (135.6 mg, 1.4 mmol) and SnCl$_4$ (1.0 M in hexane, 7.5 mL, 7.5 mmol) were added. The mixture was stirred for 20 h at room temperature to form a white suspension and filtered through Celite®. The solvent of the filtrate was removed in vacuo, and the resulting pale-yellow powder was dissolved in hexane and recrystallized at −20 °C, yielding **1** as colorless crystals (1.645 g, 3.97 mmol, 58%). Because compound **1** gradually decomposes in air, storing it under inert gas is recommended. ^{1}H NMR (C$_6$D$_6$): δ 1.72 (s, $^4J_{\text{SnH}}$ = 11 Hz, 6H, CH$_3$), 0.25 (s, 18H, SiMe$_3$); ^{13}C{^{1}H} NMR (C$_6$D$_6$): δ 159.9 (4°, $^2J_{\text{SnC}}$ = 159 Hz, C$_\beta$), 131.5 (4°, $^1J_{\text{SnC}}$ = 259 Hz, C$_\alpha$), 21.2 (1°, $^3J_{119\text{SnC}}$ = 223 Hz, $^3J_{117\text{SnC}}$ = 213 Hz, CH$_3$), 0.6 (1°, $^1J_{\text{SiC}}$ = 53 Hz, $^3J_{\text{SnC}}$ = 16 Hz, SiMe$_3$); ^{29}Si{^{1}H} NMR (CDCl$_3$): δ −6.01 (SiMe$_3$); ^{119}Sn{^{1}H} NMR (C$_6$D$_6$): δ 53.2; m.p. 111 °C; Elemental analysis calcd (%) for C$_{12}$H$_{24}$Si$_2$Cl$_2$Sn: C 34.81, H 5.84; found: C 34.92, H 6.05.

3.3. Synthesis of 1-Chloro-1-tris(trimethylsilyl)silyl-2,5-trimethylsilyl-3,4-dimethylstannole **2**

To a hexane solution (10 mL) of dichlorostannole **1** (781 mg, 1.89 mmol), KSi(SiMe$_3$)$_3$ (0.20 M in hexane, 9.4 mL, 1.9 mmol) was added at −80 °C. The resulting mixture was

stirred for 18 h at room temperature and then filtered through Celite®. After removing the solvents in vacuo, the resulting yellow powder was dissolved in Et_2O. Cooling this solution at -20 °C afforded pale-yellow crystals of **2** (382 mg, 0.610 mmol, 32% yield). Because compound **2** gradually decomposes in air, storing it under inert gas is recommended. ^1H NMR (C_6D_6): δ 2.01 (s, $^4J_{SnH}$ = 5.4 Hz, 6H, CH_3), 0.40 (s, $^4J_{SnH}$ = 6.5 Hz, 18H, $SiMe_3$), 0.36 (s, $^4J_{SnH}$ = 6.5 Hz, 27H, $Si(SiMe_3)_3$); $^{13}C\{^1H\}$ NMR (C_6D_6): δ 162.0 (4°, $^2J_{119SnC}$ = 84 Hz, $^2J_{117SnC}$ = 80 Hz, C_β), 148.5 (4°, $^1J_{119SnC}$ = 149 Hz, $^1J_{117SnC}$ = 143 Hz, $^1J_{SiC}$ = 63 Hz, C_α), 23.7 (1°, $^3J_{119SnC}$ = 117 Hz, $^3J_{117SnC}$ = 113 Hz, CH_3), 3.7 (1°, $^1J_{SiC}$ = 46 Hz, $^3J_{SnC}$ = 14 Hz, $Si(SiMe_3)_3$), 2.3 (1°, $^1J_{SiC}$ = 52 Hz, $^3J_{SnC}$ = 10 Hz, $SiMe_3$); $^{29}Si\{^1H\}$ NMR ($CDCl_3$): δ -7.23 (Si(**Si**Me$_3$)$_3$), -7.24 (**Si**(SiMe$_3$)$_3$), -7.88 (SiMe$_3$); $^{119}Sn\{^1H\}$ NMR (C_6D_6): δ 101.3; m.p. 150 °C; Elemental analysis calcd (%) for $C_{21}H_{51}Si_6ClSn$: C 40.27, H 8.21; found: C 39.95, H 8.34.

3.4. Synthesis of 1-Lithio-1-tris(trimethylsilyl)silyl-2,5-trimethylsilyl-3,4-dimethylstannole 3

Lithium metal (3.2 mg, 0.46 mmol) was added to an Et_2O solution (2 mL) of chlorostannole **2** (113 mg, 0.180 mmol) at -20 °C. After stirring for 1 h, the remaining lithium was removed by filtration. After removing the solvent in vacuo, the residue was dissolved in hexane/THF. Cooling this solution to -20 °C deposited orange crystals of **3·(thf)$_3$**. Drying the crystals under reduced pressure gave off two of the three THF molecules to give **3·thf** (31.2 mg, 0.0466 mmol, 26% yield). ^1H NMR (C_6D_6): δ 3.18 (m, 4H, thf), 2.34 (s, $^4J_{SnH}$ = 16 Hz, 6H, CH_3), 1.17 (m, 4H, thf), 0.49 (s, 27H, $Si(SiMe_3)_3$), 0.48 (s, 18H, $Si(CH_3)_3$); $^{13}C\{^1H\}$ NMR (C_6D_6): δ 180.2 (4°, C_α), 156.9 (4°, C_β), 68.9 (2°, thf), 25.9 (1°, $^3J_{SnC}$ = 13 Hz, CH_3), 25.2 (2°, thf), 5.0 (1°, $^1J_{SiC}$ = 44 Hz, $Si(SiMe_3)_3$), 3.9 (1°, $^1J_{SiC}$ = 51 Hz, $^3J_{SnC}$ = 13 Hz, $SiMe_3$); $^{29}Si\{^1H\}$ NMR (C_6D_6): δ -7.6 ($Si(SiMe_3)_3$), -8.9 ($^2J_{SnSi}$ = 43.7 Hz, $Si(SiMe_3)_3$), -10.1 ($^2J_{SnSi}$ = 39.3 Hz, $SiMe_3$); $^{119}Sn\{^1H\}$ NMR (C_6D_6): δ -130.6; $^7Li\{^1H\}$ NMR (C_6D_6): δ -1.47; m.p. > 143 °C (decomp.). Although elemental analysis could not be carried out due to the instability towards moisture and oxygen, the purity of **3** was confirmed by the ^1H, $^{13}C\{^1H\}$, $^{119}Sn\{^1H\}$, $^{29}Si\{^1H\}$ and $^7Li\{^1H\}$ NMR spectra (Figures S10–S14). Satellite signals caused by Sn−C coupling could not be observed.

3.5. Details for X-ray Diffraction Studies

Diffraction data for **2** and **3·(thf)$_3$** were collected on a VariMax Saturn CCD diffractometer with graphite-monochromated Mo Kα radiation (λ = 0.71075 Å) at -180 °C. Intensity data were corrected for Lorenz-polarization effects and for empirical absorption (REQAB). All calculations were performed using the CrystalStructure 4.3 crystallographic software package, except for refinements, which were performed using SHELXL-2018/3 [52]. The positions of the non-hydrogen atoms were determined by SHELXT [53]. All non-hydrogen atoms were refined on $F_o{}^2$ anisotropically by full-matrix least-squares techniques. All hydrogen atoms were placed at the calculated positions with fixed isotropic parameters.

Crystal data for $C_{21}H_{51}ClSi_6Sn$ (**2**) (M = 626.29 g/mol): monoclinic, space group $P2_1/c$ (no. 14), a = 18.826(2) Å, b = 28.856(3) Å, c = 18.810(2) Å, α = 90°, β = 97.7770(10)°, γ = 90°, V = 10,124.5(19) Å^3, Z = 12, T = 93(2) K, μ(MoKα) = 0.71075 mm^{-1}, D_{calc} = 1.233 g/cm^3, 82,916 reflections measured (6.0° $\leq$ 2θ $\leq$ 53.0°), 23,037 unique reflections (R_{int} = 0.0729), which were used in all calculations. The final R_1 was 0.0619 (I > 2σ(I)), wR_2 was 0.1272 (all data), and GOF = 1.128.

Crystal data for $C_{33}H_{75}LiO_3Si_6Sn$ **[3·(thf)$_3$]** (M = 814.10 g/mol): monoclinic, space group $P2_1/n$ (no. 14), a = 13.3363(11) Å, b = 19.6417(18) Å, c = 17.7954(16) Å, α = 90°, β = 91.4530(10)°, γ = 90°, V = 4660.0(7) Å^3, Z = 4, T = 93(2) K, μ(MoKα) = 0.71075 mm^{-1}, D_{calc} = 1.160 g/cm^3, 37,674 reflections measured (6.0° $\leq$ 2θ $\leq$ 55.0°), 10,667 unique reflections (R_{int} = 0.0437), which were used in all calculations. The final R_1 was 0.0437 (I > 2σ(I)), wR_2 was 0.0952 (all data), and GOF = 1.102.

4. Conclusions

We successfully synthesized novel 1,1-dichloro-2,5-disilylstannole **1**, monochlorostannole **2**, and lithium salt of stannolyl anion **3·(thf)₃** that adopts an η^1-coordination in the solid-state. Unlike the aromatic 2,5-disilylated silolyl and germolyl anions, the tin counterpart **3·(thf)₃** is concluded to be nonaromatic based on the $C-C$ bond alternation and pyramidal tin center. This conclusion is further supported by $^{119}Sn\{^1H\}$ and $^7Li\{^1H\}$ NMR spectroscopic properties. This result can be explained by a trend where the energy difference between pyramidalized metallolyl anions and the planar ones increases as the group 14 metal becomes heavier [54].

References

1. Saito, M. Transition-Metal Complexes Featuring Dianionic Heavy Group 14 Element Aromatic Ligands. *Acc. Chem. Res.* **2018**, *51*, 160–169. [CrossRef]
2. Wei, J.; Zhang, W.-X.; Xi, Z. The aromatic dianion metalloles. *Chem. Sci.* **2018**, *9*, 560–568. [CrossRef]
3. Kuwabara, T.; Saito, M. 3.17—Siloles, Germoles, Stannoles, and Plumboles. In *Comprehensive Heterocyclic Chemistry IV*; Black, D.S., Cossy, J., Stevens, C.V., Eds.; Elsevier: Oxford, UK, 2022; pp. 798–832.
4. Sun, X.; Roesky, P.W. Group 14 metallole dianions as η^5-coordinating ligands. *Inorg. Chem. Front.* **2023**, *10*, 5509–5516. [CrossRef]
5. Freeman, W.P.; Tilley, T.D.; Rheingold, A.L.; Ostrander, R.L. A Stable η^5-Germacyclopentadienyl Complex: $[(\eta^5\text{-}C_5Me_5)Ru\{\eta^5\text{-}C_4Me_4GeSi(SiMe_3)_3\}]$. *Angew. Chem. Int. Ed. Engl.* **1993**, *32*, 1744–1745. [CrossRef]
6. Freeman, W.P.; Tilley, T.D.; Rheingold, A.L. Stable Silacyclopentadienyl Complexes of Ruthenium: $(\eta^5\text{-}C_5Me_5)Ru[\eta^5\text{-}Me_4C_4SiSi(SiMe_3)_3]$ and X-ray Structure of Its Protonated Form. *J. Am. Chem. Soc.* **1994**, *116*, 8428–8429. [CrossRef]
7. Dysard, J.M.; Tilley, T.D. η^5-Silolyl and η^5-Germolyl Complexes of d^0 Hafnium. Structural Characterization of an η^5-Silolyl Complex. *J. Am. Chem. Soc.* **1998**, *120*, 8245–8246. [CrossRef]
8. Dysard, J.M.; Tilley, T.D. Synthesis and Reactivity of η^5-Silolyl, η^5-Germolyl, and η^5-Germole Dianion Complexes of Zirconium and Hafnium. *J. Am. Chem. Soc.* **2000**, *122*, 3097–3105. [CrossRef]
9. Dysard, J.M.; Tilley, T.D. Hafnium–Rhodium and Hafnium–Iridium Heterobimetallic Complexes Featuring the Bridging Germole Dianion Ligand $[GeC_4Me_4]^{2-}$. *Organometallics* **2000**, *19*, 2671–2675. [CrossRef]
10. Freeman, W.P.; Dysard, J.M.; Tilley, T.D.; Rheingold, A.L. Synthesis and Reactivity of η^5-Germacyclopentadienyl Complexes of Iron. *Organometallics* **2002**, *21*, 1734–1738. [CrossRef]
11. Kuwabara, T.; Guo, J.-D.; Nagase, S.; Sasamori, T.; Tokitoh, N.; Saito, M. Synthesis, Structures and Electronic Properties of Triple- and Double-decker Ruthenocenes Incorporated by A Group 14 Metallole Dianion Ligand. *J. Am. Chem. Soc.* **2014**, *136*, 13059–13064. [CrossRef] [PubMed]
12. Saito, M.; Nakada, M.; Kuwabara, T.; Owada, R.; Furukawa, S.; Narayanan, R.; Abe, M.; Hada, M.; Tanaka, K.; Yamamoto, Y. Inverted Sandwich Rh Complex Bearing a Plumbole Ligand and Its Catalytic Activity. *Organometallics* **2019**, *38*, 3099–3103. [CrossRef]
13. Nakada, M.; Kuwabara, T.; Furukawa, S.; Hada, M.; Minoura, M.; Saito, M. Synthesis and reactivity of a ruthenocene-type complex bearing an aromatic π-ligand with the heaviest group 14 element. *Chem. Sci.* **2017**, *8*, 3092–3097. [CrossRef] [PubMed]
14. Kuwabara, T.; Saito, M. Synthesis of a Stannole Dianion Complex Bearing a μ-η^1;η^1-Coordination Mode: Different Electronic State of Stannole Dianion Ligands Depending on Their Hapticity. *Organometallics* **2015**, *34*, 4202–4204. [CrossRef]

15. Cramer, H.H.; Bührmann, L.; Schmidtmann, M.; Müller, T. A phenyl-substituted germole dianion and its reaction with hafnocene dichloride. *Mendeleev Commun.* **2022**, *32*, 46–48. [CrossRef]

16. Dong, Z.; Janka, O.; Kösters, J.; Schmidtmann, M.; Müller, T. A Dimeric η^1,η^5-Germole Dianion Bridged Titanium(III) Complex with a Multicenter Ti−Ge−Ge−Ti Bond. *Angew. Chem. Int. Ed.* **2018**, *57*, 8634–8638. [CrossRef] [PubMed]

17. Fekete, C.; Mokrai, R.; Bombicz, P.; Nyulászi, L.; Kovács, I. η^1-silolyl-FeCp(CO)$_2$ complexes. Is there a way to sila-ferrocene? *J. Organomet. Chem.* **2015**, *799–800*, 291–298. [CrossRef]

18. Kuwabara, T.; Nakada, M.; Guo, J.D.; Nagase, S.; Saito, M. Diverse coordination modes in tin analogues of a cyclopentadienyl anion depending on the substituents on the tin atom. *Dalton Trans.* **2015**, *44*, 16266–16271. [CrossRef]

19. Liu, J.; Singh, K.; Dutta, S.; Feng, Z.; Koley, D.; Tan, G.; Wang, X. Yttrium germole dianion complexes with Y–Ge bonds. *Dalton Trans.* **2021**, *50*, 5552–5556. [CrossRef]

20. Sun, X.; Münzfeld, L.; Jin, D.; Hauser, A.; Roesky, P.W. Silole and germole complexes of lanthanum and cerium. *Chem. Commun.* **2022**, *58*, 7976–7979. [CrossRef]

21. Münzfeld, L.; Sun, X.; Schlittenhardt, S.; Schoo, C.; Hauser, A.; Gillhuber, S.; Weigend, F.; Ruben, M.; Roesky, P.W. Introduction of plumbole to f-element chemistry. *Chem. Sci.* **2022**, *13*, 945–954. [CrossRef] [PubMed]

22. De, S.; Mondal, A.; Ruan, Z.-Y.; Tong, M.-L.; Layfield, R.A. Dynamic Magnetic Properties of Germole-ligated Lanthanide Sandwich Complexes. *Chem. Eur. J.* **2023**, *29*, e202300567. [CrossRef]

23. Freeman, W.P.; Tilley, T.D.; Yap, G.P.A.; Rheingold, A.L. Silolyl Anions and Silole Dianions: Structure of [K([18]crown-6)$^+$]$_2$[C$_4$Me$_4$Si^{2-}]. *Angew. Chem. Int. Ed. Engl.* **1996**, *35*, 882–884. [CrossRef]

24. West, R.; Sohn, H.; Bankwitz, U.; Calabrese, J.; Apeloig, Y.; Mueller, T. Dilithium Derivative of Tetraphenylsilole: An η^1-η^5 Dilithium Structure. *J. Am. Chem. Soc.* **1995**, *117*, 11608–11609. [CrossRef]

25. Szathmári, B.; Fekete, C.; Kelemen, Z.; Holczbauer, T.; Nyulászi, L.; Kovács, I. Synthesis of Silolide Dianions via Reduction of Dichlorosiloles: Important Role of the Solvent. *Eur. J. Inorg. Chem.* **2023**, *26*, e202300316. [CrossRef]

26. Dong, Z.; Reinhold, C.R.W.; Schmidtmann, M.; Müller, T. Trialkylsilyl-Substituted Silole and Germole Dianions. *Organometallics* **2018**, *37*, 4736–4743. [CrossRef]

27. West, R.; Sohn, H.; Powell, D.R.; Müller, T.; Apeloig, Y. The Dianion of Tetraphenylgermole is Aromatic. *Angew. Chem. Int. Ed. Engl.* **1996**, *35*, 1002–1004. [CrossRef]

28. Choi, S.-B.; Boudjouk, P.; Hong, J.-H. Unique Bis-η^5/η^1 Bonding in a Dianionic Germole. Synthesis and Structural Characterization of the Dilithium Salt of the 2,3,4,5-Tetraethyl Germole Dianion. *Organometallics* **1999**, *18*, 2919–2921. [CrossRef]

29. Saito, M.; Haga, R.; Yoshioka, M.; Ishimura, K.; Nagase, S. The Aromaticity of the Stannole Dianion. *Angew. Chem. Int. Ed.* **2005**, *44*, 6553–6556. [CrossRef] [PubMed]

30. Saito, M.; Kuwabara, T.; Kambayashi, C.; Yoshioka, M.; Ishimura, K.; Nagase, S. Synthesis, Structure, and Reaction of Tetraethyldilithiostannole. *Chem. Lett.* **2010**, *39*, 700–701. [CrossRef]

31. Kuwabara, T.; Guo, J.-D.; Nagase, S.; Minoura, M.; Herber, R.H.; Saito, M. Enhancement of Stannylene Character in Stannole Dianion Equivalents Evidenced by NMR and Mössbauer Spectroscopy and Theoretical Studies of Newly Synthesized Silyl-Substituted Dilithiostannoles. *Organometallics* **2014**, *33*, 2910–2913. [CrossRef]

32. Saito, M.; Sakaguchi, M.; Tajima, T.; Ishimura, K.; Nagase, S.; Hada, M. Dilithioplumbole: A Lead-Bearing Aromatic Cyclopentadienyl Analog. *Science* **2010**, *328*, 339–342. [CrossRef]

33. Saito, M.; Nakada, M.; Kuwabara, T.; Minoura, M. A reversible two-electron redox system involving a divalent lead species. *Chem. Commun.* **2015**, *51*, 4674–4676. [CrossRef] [PubMed]

34. Freeman, W.P.; Tilley, T.D.; Liable-Sands, L.M.; Rheingold, A.L. Synthesis and Study of Cyclic π-Systems Containing Silicon and Germanium. The Question of Aromaticity in Cyclopentadienyl Analogues. *J. Am. Chem. Soc.* **1996**, *118*, 10457–10468. [CrossRef]

35. Saito, M.; Kuwabara, T.; Ishimura, K.; Nagase, S. Synthesis and Structures of Lithium Salts of Stannole Anions. *Bull. Chem. Soc. Jpn.* **2010**, *83*, 825–827. [CrossRef]

36. Fekete, C.; Kovács, I.; Nyulászi, L.; Holczbauer, T. Planar lithium silolide: Aromaticity, with significant contribution of non-classical resonance structures. *Chem. Commun.* **2017**, *53*, 11064–11067. [CrossRef]

37. Fekete, C.; Kovács, I.; Könczöl, L.; Benkő, Z.; Nyulászi, L. Substituent effect on the aromaticity of the silolide anion. *Struct. Chem.* **2014**, *25*, 377–387. [CrossRef]

38. Dong, Z.; Schmidtmann, M.; Müller, T. Potassium Salts of 2,5-Bis(trimethylsilyl)-Germolide: Switching between Aromatic and Non-Aromatic States. *Chem. Eur. J.* **2019**, *25*, 10858–10865. [CrossRef] [PubMed]

39. Goodwin, S.D.; Wei, P.; Beck, B.C.; Su, J.; Robinson, G.H. Synthesis and Molecular Structure of Germanium and Tin Tetraphenylbutadienyl Based Heterocyclic Halides. *Main Group Chem.* **2000**, *3*, 137–141. [CrossRef]

40. Wrackmeyer, B.; Kehr, G.; Willbold, S.; Ali, S. Novel organotin halides. Organometallic substituted stannoles and alkene derivatives with tin–chlorine and tin–bromine bonds—Exceptionally small magnitude of coupling constants $|^1J(^{119}\text{Sn},^{13}\text{C})|$. *J. Organomet. Chem.* **2002**, *646*, 125–133. [CrossRef]

41. Negishi, E.-i.; Cederbaum, F.E.; Takahashi, T. Reaction of zirconocene dichloride with alkyllithiums or alkyl grignard reagents as a convenient method for generating a "zirconocene" equivalant and its use in zirconium-promoted cyclization of alkenes, alkynes, dienes, enynes, and diynes. *Tetrahedron Lett.* **1986**, *27*, 2829–2832. [CrossRef]

42. Ura, Y.; Li, Y.; Xi, Z.; Takahashi, T. Cu(I) catalyzed or promoted metallacycle transfer of zirconacycles to stannacycles. *Tetrahedron Lett.* **1998**, *39*, 2787–2790. [CrossRef]

43. Aakeröy, C.B.; Evans, T.A.; Seddon, K.R.; Pálinkó, I. The C–H···Cl hydrogen bond: Does it exist? *New J. Chem.* **1999**, *23*, 145–152. [CrossRef]

44. Reed, D.; Stalke, D.; Wright, D.S. Observation of a Direct Sn–Li Bond; The Crystal and Molecular Structure of Monomeric [Ph$_3$SnLi · PMDETA] and the Detection of ^{119}, ^{117}Sn–^{7}Li NMR Coupling in Solution. *Angew. Chem. Int. Ed. Engl.* **1991**, *30*, 1459–1460. [CrossRef]

45. Fukawa, T.; Nakamoto, M.; Lee, V.Y.; Sekiguchi, A. Structural Diversity of the Tris(di-tert-butylmethylsilyl)stannyl Anion: Monomeric vs Dimeric, Lithium Coordinated vs Lithium Free. *Organometallics* **2004**, *23*, 2376–2381. [CrossRef]

46. Nanjo, M.; Nanjo, E.; Mochida, K. Tris(trimethylsilyl)-Substituted Heavy Group 14-Element-Centered Anions: Unsolvated Trimeric Germyllithium and Solvated Dimeric Silyl- and Stannyllithiums. *Eur. J. Inorg. Chem.* **2004**, *2004*, 2961–2967. [CrossRef]

47. Ito, S.; Kuwabara, T.; Ishii, Y. A Tin Analogue of the Cycloheptatrienyl Anion: Synthesis, Structure, and Further Reduction to Form a Dianionic Species. *Organometallics* **2020**, *39*, 640–644. [CrossRef]

48. Haga, R.; Saito, M.; Yoshioka, M. Synthesis and Reactions of Stannole Anions. *Eur. J. Inorg. Chem.* **2007**, *2007*, 1297–1306. [CrossRef]

49. Narayanan, R.; Nakada, M.; Abe, M.; Saito, M.; Hada, M. ^{13}C and ^{207}Pb NMR Chemical Shifts of Dirhodio- and Dilithioplumbole Complexes: A Quantum Chemical Assessment. *Inorg. Chem.* **2019**, *58*, 14708–14719. [CrossRef]

50. Saito, M.; Yoshioka, M. The anions and dianions of group 14 metalloles. *Coord. Chem. Rev.* **2005**, *249*, 765–780. [CrossRef]

51. Marschner, C. A New and Easy Route to Polysilanylpotassium Compounds. *Eur. J. Inorg. Chem.* **1998**, *1998*, 221–226. [CrossRef]

52. Sheldrick, G. Crystal structure refinement with SHELXL. *Acta Crystallogr. Sect. C* **2015**, *71*, 3–8. [CrossRef] [PubMed]

53. Sheldrick, G. SHELXT—Integrated space-group and crystal-structure determination. *Acta Crystllogr. Sect. A* **2015**, *71*, 3–8. [CrossRef] [PubMed]

54. Goldfuss, B.; Schleyer, P.v.R. Aromaticity in Group 14 Metalloles: Structural, Energetic, and Magnetic Criteria. *Organometallics* **1997**, *16*, 1543–1552. [CrossRef]